1(c) to the linear term in the arc tan but one must also take the cubic term in the arc tan. There is a connected term of precisely the same geometry as Fig. 1(c) coming from the cube of the disconnected or two-body parts of the $K$ matrix. Here, however, intermediate states get a $\delta(E-H_0)$ rather than a $P[1/(E-H_0)]$. It is important to take these two terms together in order to get a finite answer. All other terms are higher order.

Putting the $C$ term of Eq. (6) [Fig. 1(d)] in the linearized arc tan makes a direct evaluation even more difficult, but it is again clear on dimensional grounds that there will be a term in $\bar{b}_3$ of the form $\lambda^{-4}\ln\lambda$. It has been claimed that $b_n$ contains only positive and negative integral powers of $\lambda$.[10] This does not seem to be the case.

It is clear from this analysis that terms beyond $\lambda^{-4}\ln\lambda$ in $\bar{b}_3$ require a full solution of the three-body problem since they involve terms of $O(1)$ in $E$ in Eq. (6).

Turning to the $n$-body cluster coefficient $b_n$, there will again be terms connected by statistics, which presumably can be summed into statistical corrections to lower-order terms and terms connected by scattering. It is easy to see that the leading low-energy contribution to the $n$-body $K$ matrix goes as $A/E^{n-2}$ with $A$ proportional to $a^{n-1}$. In Eq. (3) again the linear term in the arc tan will dominate. Thus one finally gets as the leading low-temperature contribution to $b_n$ from $n$-body scattering a term proportional to $(a/\lambda)^{n-1}$ (if there are no $n$-body bound states). There are terms of higher order in $1/\lambda^m$ and $(1/\lambda^m)\ln^k\lambda$, but one does not need solutions of the full $n$-body problem until one gets to terms of order $1/\lambda^{3n-5}$.

One of us (R.D.A.) would like to thank Professor Morton Rubin for many interesting discussions during the early stages of this work.

*Supported in part by the National Science Foundation.

[1]R. Dashen, S. K. Ma, and H. J. Bernstein, Phys. Rev. 187, 345 (1969).

[2]R. D. Amado and M. H. Rubin, Phys. Rev. Lett. 25, 194 (1970).

[3]Throughout this note we assume the interactions are such as to give no $n$-body bound states. If such states exist they will, of course, dominate the low-temperature dependence of $b_n$.

[4]Cf. K. Huang, *Statistical Mechanics* (Wiley, New York, 1963).

[5]R. Dashen and S. K. Ma, J. Math. Phys. 11, 1136 (1970), and 12, 689 (1971).

[6]A. Pais and G. E. Uhlenbeck, Phys. Rev. 116, 250 (1959).

[7]S. Y. Larsen and P. L. Mascheroni, Phys. Rev. A 2, 1018 (1970).

[8]Cf. T. D. Lee and C. N. Yang, Phys. Rev. 116, 25 (1959).

[9]Cf. such comments in Ref. 5.

[10]P. L. Mascheroni, Phys. Rev. Lett. 25, 726, 1148(E) (1970).

# Demonstration of Collisionless Interactions Between Interstreaming Ions in a Laser-Produced-Plasma Experiment

S. O. Dean, E. A. McLean, J. A. Stamper, and Hans R. Griem*
*Naval Research Laboratory, Washington, D. C. 20390*
(Received 11 June 1971)

Evidence has been obtained for collision-free momentum transfer between the ions of interstreaming plasmas in a laser-produced-plasma experiment. Diagnostics employed included fast photography, shadowgraphy, and electric potential probes. Spectroscopy provided direct evidence of momentum transfer from Doppler shifts of ion lines.

A high-density, high-temperature plasma is produced when a $Q$-switched laser is focused onto a small solid target. Within a few nanoseconds the thermal energy of the plasma is converted into kinetic energy of radial expansion.[1] If a low-pressure ambient gas is present, then radiation from the laser-produced plasma photoionizes the gas and the laser-produced plasma streams radially outward through the resulting ambient plasma. We report observations of momentum-transfer interactions between ions of the laser-produced plasma and ions of the ambient plasma under conditions where ordinary binary momentum-transfer collisions are negligible.

Explanation of the momentum transfer requires the existence of collective ion interactions (anomalous viscosity[2]) associated with plasma instabilities. The regime of our observations, $C_s < V < v_t$ (where $V$ is the ion streaming velocity, $C_s$

the ion sound speed, and $v_t$ the electron thermal velocity), is predicted[3] to be linearly stable in the absence of a magnetic field but unstable in the presence of a small magnetic field (just electrons tied to field lines). We find collisionless interactions even in the absence of an applied field and explain this apparent discrepancy by the fact that magnetic fields, spontaneously generated by currents in the laser-produced plasma, always exist in our experiment.[4] These fields are of the order of a kilogauss about 0.5 cm from the target. This interpretation is strengthened by the fact that the results reported here were unaffected when a uniform magnetic field of up to 1 kG was externally applied.

The laser-produced plasma is formed by focusing a Nd-doped glass laser (60 J, 30 nsec) onto the tip of a 0.25-mm Lucite ($C_5H_8O_2$) fiber suspended in an ambient nitrogen gas. A series of framing photographs, taken for various filling pressures (32–240 mTorr) of nitrogen gas, showed a luminous region with a sharply defined boundary. The distance to which the boundary expanded in a fixed time was strongly dependent on pressure, indicating that the boundary was an interaction front with the ambient plasma. This distance was found to be inversely proportional to the cube root of the ambient pressure. Streak photographs, taken over the same range of pressures, showed that the fronts expanded with velocities of a few times $10^7$ cm/sec and then slowed down to velocities of several times $10^6$ cm/sec at times greater than 100 nsec. A typical plot of radius versus time is shown in Fig. 1.

The nature of the front was further investigated by shadowgraphy.[5] The light source for the shadowgraphy was obtained by splitting off a portion of the main laser beam (1.06 $\mu$m) and then frequency-doubling into the visible region of this spectrum. After introducing a measured optical-path delay, the beam was passed through the experimental region and allowed to fall on a photographic plate. This light is strongly refracted when it passes through regions having large gradients of electron density, such as may be present in an interaction front. The interaction front is seen in the shadowgraph shown in Fig. 2. The fiber target is also evident, as is the dense plasma core where the laser radiation is absorbed. The "bright-dark-bright" pattern in the front is indicative of a shell of enhanced electron density, as would be expected if the laser-produced plasma were acting as a piston which "snowplows" the ambient plasma. The thickness of the interaction front is approximately 1 mm. The binary-collision momentum-transfer mean free path, estimated from a screened Coulomb potential, is several centimeters.

If no interaction were occurring between the interstreaming plasmas, then the laser-produced plasma expansion velocity would be independent of ambient pressure. The observed dependence of expansion velocity on ambient pressure is shown in Fig. 3. This dependence, $V \propto p^{-1/3}$, is in agreement with the predictions of a strong momentum-transfer model, namely, the "radiation-driven detonation wave."[6] The late-time dynamics (Fig. 1), $r \propto t^{0.4}$, is also in agreement with a strong momentum-transfer model, namely the "blast-wave" model.[7]

In the absence of binary collisions, the force required for momentum transfer must come from an electric field. Electric potential probes[8,9]

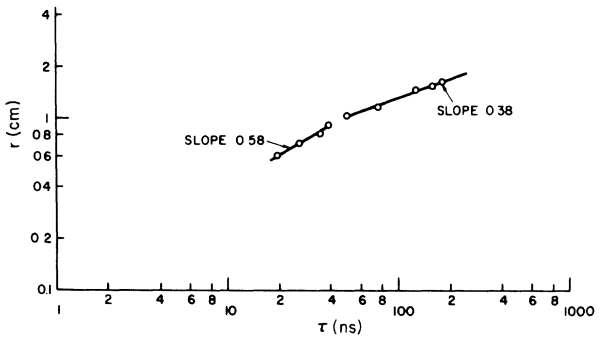


FIG. 1. Radius of luminous front versus time for 120-mTorr ambient nitrogen pressure. Laser parameters were 8 J, 30 nsec. Data are taken from 200-nsec-duration streak photographs. Time is measured from the moment the leading edge of incident laser pulse arrives at target.

FIG. 2. Shadowgraph, in 200-mTorr nitrogen, taken 53 nsec after leading edge of incident laser pulse arrives at target. Effective exposure time is approximately 5 nsec.

were used to look for the presence of electric fields in the interaction region. Potentials were observed of the order of 100 eV. This is sufficient to account for the approximately 80 eV kinetic energy imparted to a nitrogen ion during the collision-free interaction. An important feature of the data was that the rise time of the potential (6 nsec at a 5-mm radial probe position) was independent of ambient pressure at a fixed probe position. Since the front width can be defined from the electric probe data as $\delta = V\tau$, where $V$ is the velocity of the front and $\tau$ is the rise time of the potential signal, this means that the thickness depends on density only through the dependence of $V$ on density. A theory[9] for the ion-ion two-stream instability in the presence of a magnetic field predicts that $\delta = \frac{1}{6}\sqrt{6}V\omega_{pe}/\omega_{pi}\omega_{ce}$ (where $\omega_{pe}$ and $\omega_{pi}$ are the electron and ion plasma frequencies, respectively, and $\omega_{ce}$ is the electron cyclotron frequency), which likewise depends on ambient density only through the dependence of $V$ on density. The dependence of front width on density, as derived from electric probe data, agrees well with this theory, as shown in Fig. 4. This dependence is not predicted by other common expressions for collision-free widths, such as that due to ion-acoustic instability[10] ($\sim 10c/\omega_{pe}$), ion-ion two-stream instability in the absence of a magnetic field[11] ($\sim 10V/\omega_{pi}$), or ion-gyration mixing[12] and nonlinear wave-wave interactions[13] ($\sim c/\omega_{pi}$). For a typical ambient pressure of 120 mTorr, the quantities $V$, $\omega_{pe}$, $\omega_{pi}$, and $\omega_{ce}$ have the values $2\times10^7$ cm/sec, $3.7\times10^{12}$ sec$^{-1}$, $2.3\times10^{10}$ sec$^{-1}$, and $1.8\times10^{10}$ sec$^{-1}$, respectively. It is expected that the numerical values of the experimental and theoretical thicknesses should agree only in order of magnitude.

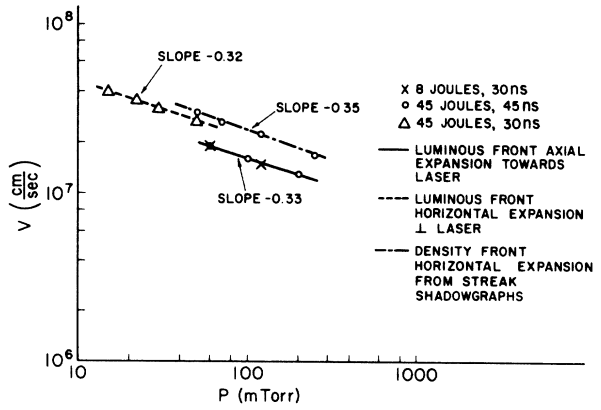


FIG. 3. Initial fast expansion velocity (see Fig. 1) of laser-produced plasma versus ambient nitrogen pressure.

Direct evidence for momentum transfer from the laser-produced plasma to the ambient nitrogen ions was obtained by spectroscopic observations of Doppler-shifted nitrogen ion lines as shown in Fig. 5. Observations of the luminous front were made along the line of sight perpendicular to the laser beam and 8 mm to the laser side of the target. These data, taken in a shot-to-shot scan, assuming reproducibility of the phenomena, revealed weak "satellite" lines[14] on the wings of strong N II lines.

Since strong lines nearby prevented observations of both wings of any *one* N II line, the red wing of N II 4621 and the blue wing of N II 4631 were scanned. The unshifted peak intensities of N II 4631 and N II 4621 were at least 10 times greater than their satellite lines.

It is noted in Fig. 5 that the peak of the N II 4631 satellite line is shifted 2.65 Å toward the blue from the line center. This corresponds to an ion velocity of $1.75\times10^7$ cm/sec, compared with the measured luminous velocity toward the observer, $V_-$, of $2.3\times10^7$ cm/sec. The peak of the N II 4621 satellite line is shifted 1.85 Å toward the red from the line center. This corresponds to an ion velocity of $1.25\times10^7$ cm/sec compared with the measured luminous velocity away from the observer, $V_+$, of $1.4\times10^7$ cm/sec.

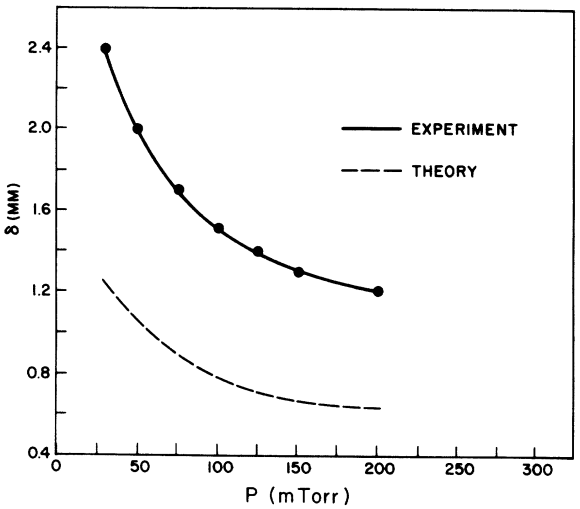


FIG. 4. Front thickness $\delta$ at a radius of 5 mm deduced from measured front velocity $V$ and measured rise time $\tau$ of electric potential ($\delta \equiv V\tau$). Lower curve which shows comparison with theory is derived by computing $\omega_{ce}$ using the value of spontaneous magnetic field $B = 1000$ G, as measured at a radius of 5 mm. The most important feature of the comparison is the functional dependence of thickness on ambient density.

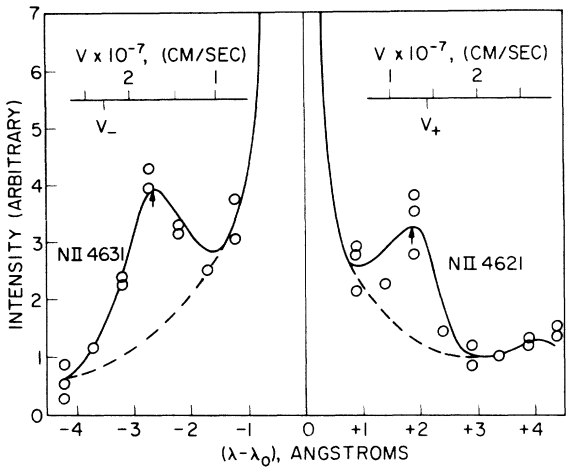


FIG. 5. Doppler-shifted satellite spectral lines on the wings of two nitrogen ion lines. The curve shown is an average of the experimental points. (The measurement could not be made on both wings of one line because of nearby impurity lines.) Conditions: pressure = 100 mTorr $N_2$, observation distance = 8 mm from target, time = 70 nsec after laser first strikes the Lucite fiber target, spectrograph slit function = 0.6 Å. The velocity scale at the top of the graph corresponds to particle velocities toward and away from the observer that would produce the corresponding spectral line shifts. The luminous front velocities measured with a streak camera are indicated as $V_-$ and $V_+$. The arrows indicate the centers of gravity of the satellite lines, determined after subtraction of the background (dashed curve) from the main lines.

Thus both the Doppler shift and the luminous front measurements of velocity show a similar asymmetry in the expansion. It is concluded from these data that the background ions are swept up by the luminous front and given approximately the velocity of the front.[15]

We wish to acknowledge the technical assistance of J. W. Cheadle, Jr., and T. H. DeRieux.

*Permanent address: Department of Physics and Astronomy, University of Maryland, College Park, Md. 20742.

[1]J. M. Dawson, Phys. Fluids 7, 981 (1964).

[2]A. G. Es'kov, R. K. Kurtmullaev, A. I. Malyutin, V. I. Pil'skii, and V. N. Senemov, Zh. Eksp. Teor. Fiz. 56, 1480 (1969) [Sov. Phys. JETP 29, 793 (1969)].

[3]K. Papadopoulos, R. C. Davidson, J. M. Dawson, I. Haber, D. A. Hammer, N. A. Krall, and R. Shanny, Phys. Fluids 14, 849 (1970).

[4]J. A. Stamper, K. Papadopoulos, R. N. Sudan, S. O. Dean, E. A. McLean, and J. M. Dawson, Phys. Rev. Lett. 26, 1012 (1971).

[5]F. C. Jahoda, E. M. Little, W. E. Quinn, F. L. Ribe, and G. A. Sawyer, J. Appl. Phys. 35, 2351 (1964).

[6]S. A. Ramsden and P. Savic, Nature 203, 1217 (1964).

[7]Ya. B. Zeldovich and Yu. P. Raizer, *Physics of Shock Waves and High Temperature Hydrodynamic Phenomena* (Academic, New York, 1966), Vol. I, p. 93.

[8]J. W. M. Paul, L. S. Holmes, M. J. Parkinson, and J. Sheffield, Nature 208, 133 (1965).

[9]A. E. Robson and J. Sheffield, in *Plasma Physics and Controlled Nuclear Fusion Research* (International Atomic Energy Agency, Vienna, Austria, 1969), Vol. I, p. 119.

[10]R. Z. Sagdeev, in *Reviews of Plasma Physics*, edited by M. A. Leontovich (Consultants Bureau, New York, 1966), Vol. 4, Chap. 2.

[11]D. A. Tidman, Phys. Fluids 10, 547 (1967).

[12]P. Auer, H. Hurwitz, and R. Kilb, Phys. Fluids 5, 298 (1962).

[13]M. Camac, A. R. Kantrowitz, M. Litvak, R. M. Patrick, and H. E. Petschek, Nucl. Fusion Suppl., Part 2, 423 (1962).

[14]A similar effect was seen by W. F. Dove, in a $\theta$-pinch experiment, to be published.

[15]Evidence, deduced from optical diagnostics, for a magnetic-field–dependent interaction has also been reported by H. W. Friedman and R. M. Patrick, Bull. Amer. Phys. Soc. 15, 1449 (1970). In their experiment an aluminum plasma from a coaxial plasma gun streams about 30 cm through photoionized air. Direct evidence for ambient ion pickup was not obtained and a theoretical interpretation was not presented.

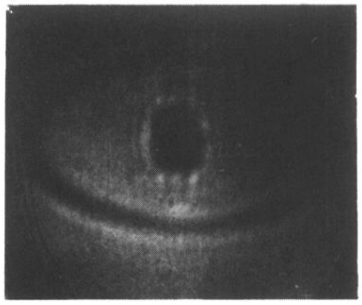

FIG. 2. Shadowgraph, in 200-mTorr nitrogen, taken 53 nsec after leading edge of incident laser pulse arrives at target. Effective exposure time is approximately 5 nsec.